nature astronomy

Article

https://doi.org/10.1038/s41550-023-02185-5

Detection of apatite in ferroan anorthosite indicative of a volatile-rich early lunar crust

Received: 31 August 2022

Accepted: 15 December 2023

Published online: 15 January 2024

Check for updates

Tara S. Hayden[1,2] ✉, Thomas J. Barrett[1,3], Mahesh Anand[1], Martin J. Whitehouse[4], Heejin Jeon[4], Xuchao Zhao[1] & Ian A. Franchi[1]

Determination of the systematics of volatile elements (for example, H, Cl, S) of the early Moon is one of the main objectives of lunar science. This has been hindered by the lack of the main volatile-bearing mineral, apatite, in ferroan anorthosites (FANs), which are thought to represent the primary products of the lunar magma ocean and the earliest lunar crust. Due to the absence of apatite, plagioclase and bulk samples of the FAN suite have been previously utilized for the studies of volatiles in samples representing the earliest-formed lunar crust. Here we provide evidence of apatite in a FAN clast in the lunar meteorite Arabian Peninsula 007. We report that Arabian Peninsula 007 has an ancient age, comparable to those of Apollo FAN samples, with lighter hydrogen ($\delta D = -45‰$) and heavier chlorine ($\delta^{37}Cl = +44‰$) isotopic compositions than FAN bulk and plagioclase data. These results suggest that the early lunar crust was significantly more volatile rich than previously thought.

Following the giant impact formation of the Moon[1], the lunar precursor material remained in a molten state for a period of between 20 and 200 Myr (ref. 2). Intense heating during the collision followed by large-scale evaporation during the lunar magma ocean (LMO) phase is thought to have depleted the Moon of volatile elements (for example, H, S, Cl) and triggered substantial fractionation of their stable isotopes (see, for example, refs. 2,3). The connected history of volatile elements on the Moon and Earth highlights their crucial importance to understanding the history of volatiles on Earth[4]. As a consequence of the lack of an atmosphere and terrestrial weathering, the Moon provides a well preserved record of events, processes and volatile composition and distribution in the inner solar system since its formation (>4.4 billion years ago, Ga)[5].

Towards the end of an extended LMO stage, the fractional crystallization of the Moon produced a dense cumulate pile comprised mainly of pyroxene and olivine and a plagioclase flotation crust, which prevented further loss of volatiles[6,7]. This flotation crust is mainly represented in the Apollo sample suite by FAN material, with later intrusive lithologies such as the Mg- and alkali suites forming in response to cumulate overturn in the lunar mantle[2,8–10] and melting at the crust–mantle boundary, respectively[11–13]. Ferroan anorthosites (FANs) are the only lithology on the Moon thought to be a primary product of the LMO[5,14]. Towards the end of LMO crystallization, the late-stage residual melt, enriched in K, rare-earth elements (REEs) and P (termed urKREEP), resided between the crust and mantle—although its geographic extent on the Moon is unclear[5]. A large proportion of the Apollo suite samples have a notable KREEP component, and hence observations of their volatile abundances and compositions may largely reflect the KREEP reservoir[15].

F, Cl and OH form essential structural constituents (ESCs) of lunar apatite, $Ca_5(PO_4)_3(F, Cl, OH)$—which is the only mineral group on the Moon identified with OH as an ESC that has been detected and studied in various lunar samples[16]. Apatite has thus far been identified in all lunar sample types except FANs and volcanic glass beads[17], as the former are thought to have formed before apatite saturation in the LMO and apatite has not been reported as inclusions in volcanic glass beads. This has limited the study of the volatile inventory of the earliest lunar crust to nominally anhydrous minerals (for example, plagioclase)[18] and bulk-rock samples[19]. The extremely low volatile abundances of nominally anhydrous minerals make stable isotope analysis challenging

[1]School of Physical Sciences, The Open University, Milton Keynes, UK. [2]Department of Earth Sciences, University of Western Ontario, London, Ontario, Canada. [3]Center for Lunar Science and Exploration, Lunar and Planetary Institute, Houston, TX, USA. [4]Department of Geosciences, Swedish Museum of Natural History, Stockholm, Sweden. ✉e-mail: tara.hayden1@open.ac.uk

https://doi.org/10.1038/s41550-023-02185-5

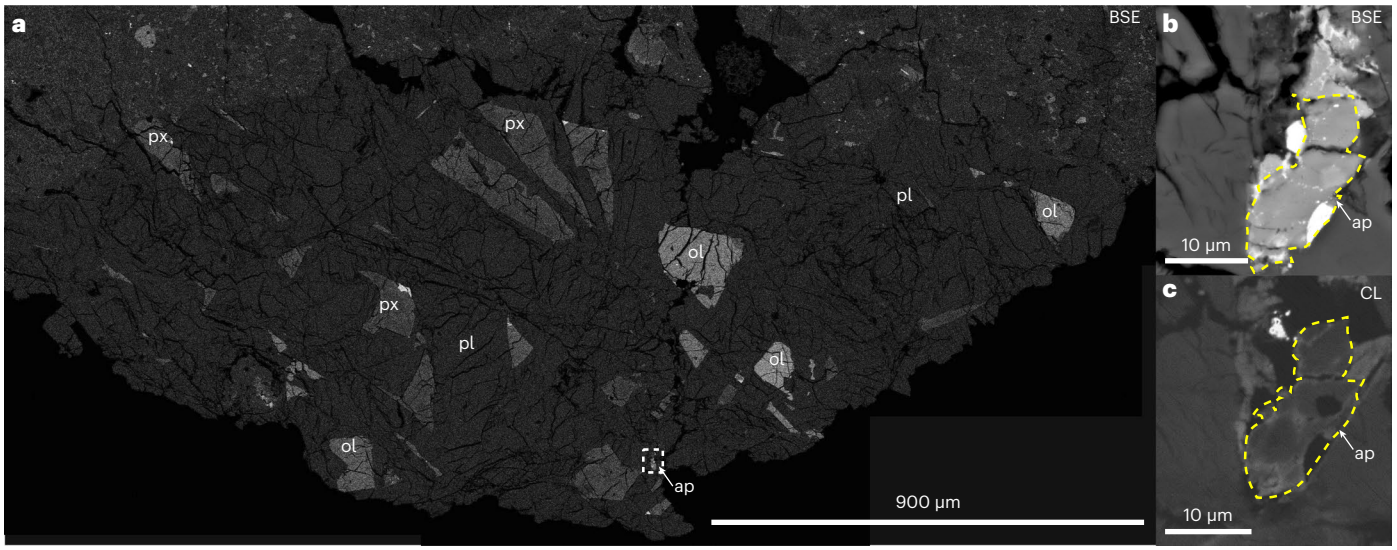

Fig. 1 | Texture of the FAN clast and associated apatite. a, Backscattered electron (BSE) map of the FAN clast in AP 007. **b**,**c**, BSE (**b**) and CL (**c**) images of apatite in the FAN clast. ap, apatite; pl, plagioclase; px, pyroxene; ol, olivine. The white dashed lines in **a** denote the region within the FAN clast in which the apatite is located, and yellow dashed lines in **b**,**c** outline the grain boundaries of the apatite.

and increase the effects of cosmic-ray spallation on δD values, while the relationship between bulk-rock and apatite δ^{37}Cl values is poorly understood, and thus bulk-rock isotopic analyses may not be entirely representative[20]. These studies of FAN material have reported that Cl and H are moderately to heavily fractionated (δ^{37}Cl = +11–30‰ (ref. 19); δD = +280–310‰ (ref. 18)). In this Article we report on observations of apatite in a FAN clast in lunar meteorite Arabian Peninsula (AP) 007 and the abundance and isotopic composition of Cl and H, as well as U–Pb and Pb–Pb chronology and Ce abundance in this apatite.

Arabian Peninsula 007

AP 007 was discovered by meteorite hunters in Al Jouf, Saudi Arabia, in 2015, as a single weathered stone lacking a fusion crust[21]. Its texture, mineral chemistry and oxygen isotope composition confirm a lunar origin (Supplementary Fig. 1). AP 007 is a clast-rich fragmental breccia, containing granulitic and recrystallized impact melt clasts enclosed in a dark, fragmental matrix. A coarse-grained crystalline clast, bearing plagioclase ($An_{95–97}$), olivine ($Fo_{44–63}$) and pyroxene ($En_{23–67}Wo_{6–44}Fs_{21–38}$), appears to be of the FAN suite (Supplementary Fig. 2) and contains apatite, ilmenite and ulvöspinel (Fig. 1). The modal abundances of plagioclase (~76%), olivine (6%) and pyroxene (17%) are similar to those of the mafic magnesian FAN subgroup[22]. The higher abundance of mafic silicates in AP 007 (and some other FAN samples) could indicate that they originate from shallower levels in lunar crustal stratigraphy[14]. Plagioclase in this clast shows strong zoning in cathodoluminescence (CL) imaging (Supplementary Fig. 3), indicating a prolonged cooling period consistent with a crustal origin and previously observed FAN material (see, for example, ref. 23). The texture of apatite is consistent with a primary magmatic origin (Supplementary Section 1.4).

The FAN suite is representative of the early lunar crust, and these samples have previously been reported to have ancient ages (Supplementary Fig. 4). Analysis of this clast yields a terrestrial common Pb-corrected $^{207}Pb/^{206}Pb$ age between 4,467 ± 43 and 4,540 ± 34 Myr (the latter value is data acquired on apatite; Supplementary Section 1.3 and Supplementary Fig. 5). This date is older than has been observed in most lunar material so far (with a similar age to Apollo FAN sample 67016; Supplementary Fig. 4), although there has been some evidence for a pre-4.5 Ga formation for the Moon[24]. FAN samples have radiometric ages of ~4.3–4.5 Gyr (refs. 24,25). It should be noted that the trend towards a radiogenic lunar Pb component introduces some dating ambiguities (Supplementary Fig. 6). Papanastassiou and Wasserburg[26,27] measured Rb–Sr ages of 4.55 ± 0.10 Gyr for Apollo dunite 72417 and 4.54 ± 0.07 Gyr in troctolite 76535, while Norman et al.[14] found a Sm–Nd age for the lunar crust of 4,456 ± 40 Myr. An age of 4,467–4,540 Myr supports previous work, which proposed crystallization of the lunar crust within ~60 Myr of calcium–aluminium-rich inclusions[14,28,29]. This evidence places the formation of this clast in AP 007 very early in the Moon's history and among the earliest FAN samples. Analysis of the volatile systematics of this early crustal material may provide greater insight into the evolution of volatiles at this stage in the early Solar System history.

Results

The δ^{37}Cl measured in this apatite is heavily fractionated (~+44.2 ± 2.2‰, 2σ), with a high Cl abundance (~1.64 ± 0.09 wt%; Supplementary Fig. 7). This is significantly heavier than bulk data observed in Apollo FAN samples 60015 (+10.5–11.4‰)[19] and 60025 (δ^{37}Cl = +24.5–30.2‰ (ref. 19); Fig. 2a) and in most other lunar material (Supplementary Fig. 8a and discussion in Supplementary Section 1.5). The δ^{37}Cl values in 60025 were attributed to significant degassing during the slow cooling of the FAN material[19]. Through back-calculation of the Ce abundance of the parental melt (~250 ppm) from that of apatite (~540 ppm), there is some similarity to more evolved endmembers of the FAN subgroups (Supplementary Section 1.7), which have been shown to not represent KREEP contamination[14].

The δD measured in this apatite is ~−45 ± 45‰ with a moderately high equivalent H_2O content (~2,300 ± 100 ppm). This δD value is comparable to those of Apollo highlands and KREEP samples (Supplementary Fig. 8b and discussion in Supplementary Section 1.5). This is lighter than observed in plagioclase within Apollo FAN samples 15415 (δD = +280‰) and 60015 (δD = +310‰; Fig. 2b), although the result for 15415 is subject to very large uncertainties (500‰), in part owing to the low H_2O content in plagioclase[18].

Discussion

It is conceivable that the Cl signature in AP 007 reflects degassing before apatite formation; this would be expected to cause a depletion in Cl in its parental melt. Rayleigh fractionation modelling of chlorine isotopes during degassing from an initial δ^{37}Cl of 0‰ requires >92% degassing of main metal chlorides (for example, $FeCl_2$, NaCl and $ZnCl_2$) to reach the δ^{37}Cl values observed here. Wang et al.[30] proposed that substantial degassing of the LMO before lunar crust formation caused a heavy

https://doi.org/10.1038/s41550-023-02185-5

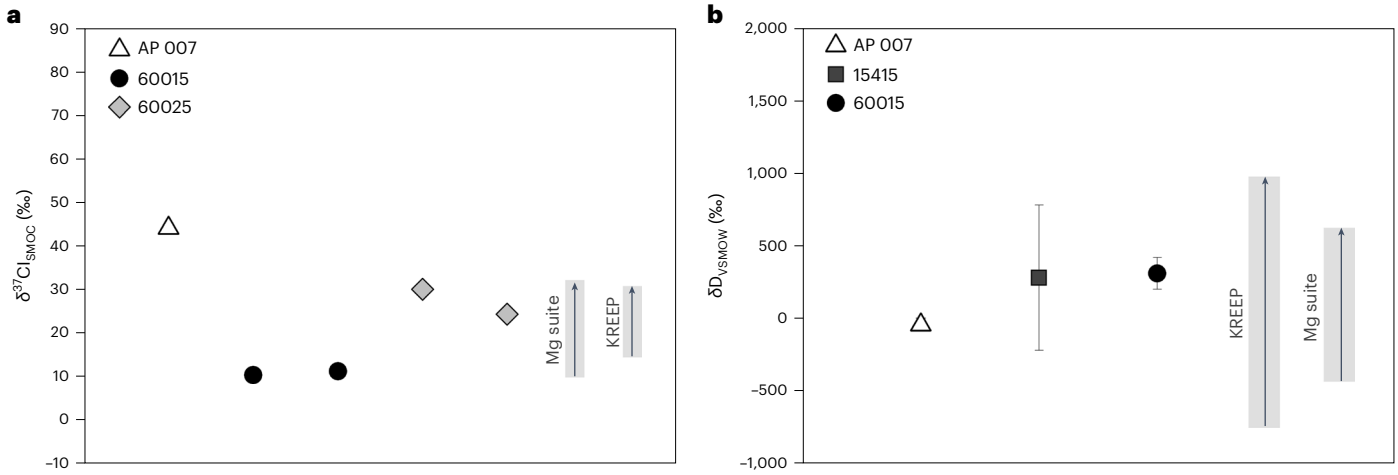

Fig. 2 | δ^{37}Cl and δD values on AP 007. a, δ^{37}Cl. **b**, δD. The values are compared with literature bulk and plagioclase in situ data on FANs[18,19], KREEP[15,42,46–48] and the Mg suite[18,37,46,49–51]. Standard error 2σ uncertainties on AP 007 data are smaller than the symbols, and are not reported for 60015 and 60025[19]. Data on AP 007 are presented as exact values ± 2σ. Data on 15415, 60015 and 60025 are presented as mean values ± 2 s.d. Data on Mg-suite and KREEP are presented as a range.

^{37}Cl enrichment. The δ^{37}Cl in AP 007 is greater than KREEP values (Fig. 2)—indicating that the fractionation observed in this sample cannot be primarily attributed to KREEP contamination, and thus other processes must be explored.

A similar enrichment in ^{37}Cl (δ^{37}Cl = +40.0 ± 2.9‰) has been attributed in Apollo 14 basalts to vapour phase metasomatism following an impact[31], and in bulk FAN samples 60015 and 60025 to condensation/metasomatism of a HCl vapour following LMO degassing[19]. Metasomatism via an evolved liquid would be expected to enrich these crustal anorthosites in REEs[32]. The observed apatite and reconstructed parental melt Ce abundances (<300 ppm) do not support metasomatism (Supplementary Section 1.7). The relatively light H isotopic composition further challenges a metasomatic origin for this apatite grain, due to the predominance of the heavier isotope in aqueous fluids and vapour phases. A lack of disturbance to the strong zoning observed in plagioclase of this clast (Supplementary Fig. 3) also indicates minimal impact interference to the rock after it solidified. This indicates that alteration of the Cl and H isotopes must have occurred before the crystallization of the rock: for example, via magmatic degassing.

Assuming a primordial δD value of −280‰, which is consistent with observations in other isotopic systems (for example, Ti and Cr, which both show an enstatite chondrite contribution to the early Moon[33]) and comparable to the proto-Earth's mantle (see, for example, ref. 34) and CI, CO and CM chondrites[35], >96% degassing of H_2 and >99% degassing of H_2O are required to raise the δD of LMO residual magmas to +310‰ (reported δD value of Apollo FAN 60015)[18]. In comparison, ~80% degassing of H_2 and >99% of H_2O is required to produce a δD of −45‰. Hui et al.[18] concluded that H_2 degassing during LMO crystallization controlled the hydrogen isotope composition of the residual melt, in agreement with our results. Degassing of H_2 followed by metal chlorides is consistent with reported volatile abundances for the LMO in the literature (Supplementary Fig. 9). It is also possible that HCl was the dominant vapour phase, in which case the aforementioned condensation and metasomatism could produce the fractionated δD values observed in AP 007. However, this is not consistent with the observed REE abundances in AP 007, and therefore should be discounted (Supplementary Section 1.6). The H_2O content of this apatite is significantly higher than estimates of the bulk silicate Moon (~130–300 ppm H_2O[36]), which may be a function of partitioning of volatiles into apatite[37]. This FAN clast is of a comparable age to other FAN suite samples (Supplementary Fig. 2), indicating that H fractionation was induced early in the lunar evolution. Through modelling of volatile contents in the LMO (Supplementary Section 1.6), the H and Cl isotopic compositions seen in AP 007 are most consistent with an initial H_2O content of <10 ppm. The results for AP 007 suggest that a significant fractionation of volatiles preceded the complete crystallization of the dry LMO. This could prompt further investigation of the Cl and H isotopes of younger lunar material to recontextualize lunar volatile history.

In this Article we have presented the in situ abundance and isotopic composition of Cl and H in apatite within a FAN clast in AP 007. The identification of apatite in this rock suite provides an insight into the volatile systematics of primary products of the LMO. It also highlights the importance of lunar meteorites in sampling lunar geology/volatiles. Isotopic measurements are supplemented by U–Pb and Pb–Pb chronology and Ce abundance measurements. An ancient ^{207}Pb/^{206}Pb age for this clast indicates that fractionation of volatiles occurred very early in lunar history, likely prior to the complete crystallization of the LMO.

Methods

We conducted a systematic search for apatite grains in thin sections of AP 007, which allowed for the identification of grains sufficiently large (at least ~10 × 10 μm^2) for nanoscale secondary-ion mass spectrometry (NanoSIMS) analysis at a high spatial resolution, and high-precision U–Pb chronology using in situ SIMS dating methods. Apatite grains were identified using BSE images and X-ray spectra using a FEI Quanta 200 three-dimensional scanning electron microscope at The Open University at accelerating voltages of 15–20 kV and a beam current of 0.60 nA. One apatite grain was found to be associated with a FAN clast with an anhedral habit and appearing interstitially between larger silicate minerals (mainly plagioclase; Fig. 1). Quantitative geochemistry of both the silicate and phosphate phases was collected using a CAMECA SX100 electron microprobe at The Open University, at accelerating voltages of 10–20 kV and beam currents of 4–20 nA. Phosphate phases were examined at higher beam currents (~10–20 nA) following NanoSIMS data collection, to remove the possibility of high probe beam currents affecting the accuracy of SIMS measurements (as electron-probe microanalysis currents would potentially mobilize the volatiles in the apatite grain)[38].

The Cl content and isotopic composition and Ce abundance of apatite grains were measured using the CAMECA NanoSIMS 50L at The Open University, following a modified protocol by Stephant et al.[39] (Supplementary Table 1). A 16 keV primary Cs^+ beam of ~50 pA was used to pre-sputter areas of either 8 × 8 μm^2 or 10 × 10 μm^2 on apatite.

Negative secondary ions of ^{13}C, ^{18}O, ^{35}Cl, ^{37}Cl, $^{40}Ca^{19}F$ and $^{140}Ce^{16}O_2$ were collected simultaneously on electron multipliers in scanning ion imaging mode, with a mass-resolving power of ~8,000 (CAMECA definition). Drift correction and data processing were carried out using the L'image software[40] developed by L. Nittler. Regions of interest over the apatite grains were selected primarily within $^{35}Cl/^{18}O$ images (Supplementary Fig. 7), allowing for the removal of signal contaminated by epoxy present in cracks and voids.

The water content (reported in this Article as equivalent H_2O; Supplementary Table 1) and hydrogen isotopes were acquired on top of existing Cl isotope image pits using the CAMECA NanoSIMS 50L in multicollection spot mode (allowing for lateral collocation of H and Cl results), refining an established protocol[41]. A 16 keV primary Cs^+ beam of ~200 pA was used to pre-sputter areas of 10 × 10 μm^2 on apatite. Negative secondary ions of ^{13}C, ^1H, ^2H and ^{18}O were collected simultaneously on electron multipliers using this primary beam, with a mass-resolving power of ~4,300 (refs. 37,42). Cosmic-ray exposure ages have not been reported for AP 007—and a whole-rock cosmic-ray exposure age would not be representative for all of the components of this complex fragmental breccia. Moreover, at the high H_2O content of apatite in AP 007, spallogenic H would not cause significant alteration of its H isotope composition (Supplementary Fig. 10). The D/H ratios and H_2O abundance of these results should, therefore, be considered as a maximum.

Bulk oxygen isotope analysis was undertaken at The Open University using infrared laser fluorination (see ref. 43 for a breakdown of this method). A 2 mg aliquot of AP 007 and standards were loaded into a Ni sample block, which was then placed in a two-part chamber, and heated under vacuum for 24 h to temperatures of at least 70 °C to ensure removal of adsorbed atmospheric moisture[44]. Further flushing and heating of the chamber using BrF_5 ensured the reduction of retained adsorbed moisture, and then the released O_2 was purified via liquid nitrogen 'cold traps'[43,44]. The O isotope composition was measured using a Thermo Fisher MAT 253 dual-inlet mass spectrometer[43,44] (see Supplementary Table 2 for results).

Statistical analyses run on the compositional data are described in Supplementary Section 1.2. Two-tailed Student *t*-tests assuming unequal variance were carried out on the electron-probe microanalysis data from AP 007 (Supplementary Tables 3 and 4).

Pb isotopes of apatite, plagioclase, olivine and pyroxene in the section (Supplementary Table 5) were measured using a CAMECA IMS 1280 ion microprobe at the NordSIMS facility in the Swedish Museum of Natural History. An Oregon Physics H201 RF plasma source generated an O_2^- Gaussian beam of about 2 nA (apatite) and 10 nA (plagioclase, olivine and pyroxene) with an impact energy of 23 kV, rastered over 5 × 5 μm^2 (apatite) or 10 × 10 μm^2 (plagioclase, olivine and pyroxene) during the analysis. Four Pb isotopes (^{204}Pb, ^{206}Pb, ^{207}Pb and ^{208}Pb) were collected simultaneously using low-noise multichannel ion counting detection, at a nominal mass resolution of 4,860 ($M/\Delta M$). Isochrons were constructed from the reported U and Pb isotope values using the Isoplot 4.1 add-in for Microsoft Excel (Berkley Geochronology Center; Supplementary Fig. 5). The overall analytical and data process procedures followed an established protocol[45].

Degassing modelling was carried out to contextualize the Cl and H isotopic compositions and abundances observed in AP 007. Rayleigh and closed system degassing modelling were carried out using the fractionation factors outlined in Supplementary Table 6. Supplementary Section 1.6 provides a detailed discussion on the effects of these degassing scenarios and the implication for the estimated H_2O and Cl contents of the LMO at the time of FAN crystallization.

The Ce abundance of the parental melt of AP 007 was reconstructed using known partition coefficient values for Ce in apatite. This was then compared with various FAN subgroups to evaluate the possible subgroup with which AP 007 may be associated (Supplementary Table 7).

Data availability

The data that support the findings in this study are available within the paper and its Supplementary Information. All other data are available from the corresponding author upon request and are publicly available at the Open Research Data Online repository under the PhD thesis data for T.S.H. The main mass (1,337 g) of AP 007 is held by D. Dickens. A type specimen (21 g) is held at The Open University (UK) by M.A.

References

1. Canup, R. M. & Asphaug, E. Origin of the Moon in a giant impact near the end of the Earth's formation. *Nature* **412**, 708–712 (2001).
2. Elkins-Tanton, L. T., Burgess, S. & Yin, Q.-Z. The lunar magma ocean: reconciling the solidifcation process with lunar petrology and geochronology. *Earth Planet. Sci. Lett.* **304**, 326–336 (2011).
3. Pahlevan, K. & Stevenson, D. J. Equilibration in the aftermath of the lunar-forming giant impact. *Earth Planet. Sci. Lett.* **262**, 438–449 (2007).
4. Righter, K. Volatile element depletion of the Moon—the roles of precursors, post-impact disk dynamics, and core formation. *Sci. Adv.* **5**, eaau7658 (2019).
5. Shearer, C. K. et al. Thermal and magmatic evolution of the Moon. *Rev. Mineral. Geochem.* **60**, 365–518 (2006).
6. Shearer, C. K. & Papike, J. J. Magmatic evolution of the Moon. *Am. Mineral.* **94**, 1469–1494 (1999).
7. Wieczorek, M. A. et al. The constitution and structure of the lunar interior. *Rev. Mineral. Geochem.* **60**, 221–364 (2006).
8. Prissel, T. C., Parman, S. W. & Head, J. W. Formation of the lunar highlands Mg-suite as told by spinel. *Am. Mineral.* **01**, 1624–1635 (2016).
9. Prissel, T. C., Whitten, J. L., Parman, S. W. & Head, J. W. On the potential for lunar highlands Mg-suite extrusive volcanism and implications concerning crustal evolution. *Icarus* **277**, 319–329 (2016).
10. Warren, P. H. The origin of pristine KREEP: effects of mixing between urKREEP and the magmas parental to the Mg-rich cumulates. In *Proc. Lunar and Planetary Science Conference* 233–241 (Cambridge Univ. Press/Lunar and Planetary Institute, 1988).
11. Elardo, S. M., Draper, D. S. & Shearer, C. K. J. Lunar Magma Ocean crystallization revisited: bulk composition, early cumulate mineralogy, and the source regions of the highlands Mg-suite. *Geochim. Cosmochim. Acta* **75**, 3024–3045 (2011).
12. Shearer, C. K., Elardo, S. M., Petro, N. E., Borg, L. E. & McCubbin, F. M. Origin of the lunar highlands Mg-suite: an integrated petrology, geochemistry, chronology, and remote sensing perspective. *Am. Mineral.* **100**, 294–325 (2015).
13. Shearer, C. K. & Papike, J. J. Early crustal building processes on the moon: models for the petrogenesis of the magnesian suite. *Geochim. Cosmochim. Acta* **69**, 3445–3461 (2005).
14. Norman, M. D., Borg, L. E., Nyquist, L. E. & Bogard, D. D. Chronology, geochemistry, and petrology of a ferroan noritic anorthosite clast from Descartes breccia 67215: clues to the age, origin, structure, and impact history of the lunar crust. *Meteorit. Planet. Sci.* **38**, 645–661 (2003).
15. Barnes, J. J. et al. Early degassing of lunar urKREEP by crust-breaching impact(s). *Earth Planet. Sci. Lett.* **447**, 84–94 (2016).
16. McCubbin, F. M. & Jones, R. H. Extraterrestrial apatite: planetary geochemistry to astrobiology. *Elements* **11**, 183–188 (2015).
17. McCubbin, F. M. et al. Magmatic volatiles (H, C, N, F, S, Cl) in the lunar mantle, crust, and regolith: abundances, distributions, processes, and reservoirs. *Am. Mineral.* **100**, 1668–1707 (2015).
18. Hui, H. et al. A heterogeneous lunar interior for hydrogen isotopes as revealed by the lunar highlands samples. *Earth Planet. Sci. Lett.* **4723**, 14–23 (2017).

19. Gargano, A. et al. The Cl isotope composotion and halogen contents of Apollo-return samples. *Proc. Natl Acad. Sci. USA* **117**, 23418–23425 (2020).
20. McCubbin, F. M. et al. Endogenous lunar volatiles. *Rev. Mineral. Geochem.* **89**, 729–786 (2023).
21. Gattacceca, J., McCubbin, F. M., Bouvier, A. & Grossman, J. N. The Meteoritical Bulletin, no. 108. *Meteorit. Planet. Sci.* **55**, 1146–1150 (2020).
22. Floss, C., James, O. B., McGee, J. J. & Crozaz, G. Lunar ferroan anorthosite petrogenesis: clues from trace element distributions in FAN subgroups. *Geochim. Cosmochim. Acta* **62**, 1255–1283 (1998).
23. Pernet-Fisher, J. F., Joy, K. H., Martin, D. & Donaldson Hanna, K. L. Assessing the shock state of the lunar highands: implications for the petrogenesis and chronology of crustal anorthosites. *Sci. Rep.* **7**, 5888 (2017).
24. Hanan, B. B. & Tilton, G. R. Relict of primitive lunar crust? *Earth Planet. Sci. Lett.* **84**, 15–21 (1987).
25. Carlson, R. W. & Lugmair, G. W. The age of ferroan anorthosite 60025: oldest crust on a young Moon? *Earth Planet. Sci. Lett.* **90**, 119–130 (1988).
26. Papanastassiou, D. A. & Wasserburg, G. J. Rb–Sr age of troctolite 76535. In *Lunar and Planetary Science Conference Proc.* Vol. 2 2035–2054 (Pergamon, 1976).
27. Papanastassiou, D. A. & Wasserburg, G. J. Rb–Sr study of a lunar dunite and evidence for early lunar differentiates. In *Lunar and Planetary Science Conference Proc.* Vol. 2 1467–1489 (Pergamon, 1975).
28. Borg, L. E., Connelly, J. N., Boyet, M. & Carlson, R. W. Chronological evidence that the Moon is either young or did not have a global magma ocean. *Nature* **477**, 70–72 (2011).
29. Touboul, M., Kleine, T., Bourdon, B., Palme, H. & Wieler, R. Late formation and prolonged differentiation of the Moon inferred from W isotopes in lunar metals. *Nature* **450**, 1206–1209 (2007).
30. Wang, Y., Hsu, W. & Guan, Y. An extremely heavy chlorine reservoir in the Moon: insights from the apatite in lunar meteorites. *Sci. Rep.* **9**, 5727 (2019).
31. Potts, N. J., Barnes, J. J., Tartèse, R., Franchi, I. A. & Anand, M. Chlorine isotopic compositions of apatite in Apollo 14 rocks: evidence for widespread vapor-phase metasomatism on the lunar nearside ~4 billion years ago. *Geochim. Cosmochim. Acta* **230**, 46–59 (2018).
32. Mercer, C. N., Treiman, A. H. & Joy, K. H. New lunar meteorite Northwest Africa 2996: a window into farside lithologies and petrogenesis. *Meteorit. Planet. Sci.* **48**, 289–315 (2013).
33. Dauphas, N., Burkhardt, C., Warren, P. H. & Fang-Zhen, T. Geochemical arguments for an Earth-like Moon-forming impactor. *Philos. Trans. R. Soc.* **372**, 20130244 (2014).
34. Hallis, L. J. et al. Evidence for primordial water in Earth's deep mantle. *Science* **350**, 795–797 (2015).
35. Alexander, C. O. D. et al. The provenances of asteroids, and their contributions to the volatile inventories of the terrestrial planets. *Science* **337**, 721–723 (2012).
36. Hauri, E. H., Saal, A. E., Rutherford, M. J. & Van Orman, J. A. Water in the Moon's interior: truth and consequences. *Earth Planet. Sci. Lett.* **409**, 252–264 (2015).
37. Barnes, J. J. et al. The origin of water in the primitive Moon as revealed by the lunar highlands samples. *Earth Planet. Sci. Lett.* **390**, 244–252 (2014).
38. Barnes, J. J. et al. Accurate and precise measurements of the D/H ratio and hydroxyl content in lunar apatites using NanoSIMS. *Chem. Geol.* **337**, 48–55 (2013).
39. Stephant, A. et al. The chlorine isotopic composition of the Moon: insights from melt inclusions. *Earth Planet. Sci. Lett.* **523**, 115715 (2019).
40. Nittler, L. L'Image Larry's Image Program (2022).
41. Barrett, T. J. et al. Exploring relationships between shock-induced microstructures and H_2O and Cl in apatite grains from eucrite meteorites. *Geochim. Cosmochim. Acta* **302**, 120–140 (2021).
42. Tartèse, R. et al. Apatite in lunar KREEP basalts: the missing link to understanding the H isotope systematics of the Moon. *Geology* **42**, 363–366 (2014).
43. Miller, M. F., Franchi, I. A., Sexton, A. S. & Pillinger, C. T. High precision $\delta^{17}O$ isotope measurements of oxygen from silicates and other oxides: method and applications. *Rapid Commun.* **13**, 1211–1217 (1999).
44. Greenwood, R. C. et al. Oxygen isotopic evidence for accretion of Earth's water before a high-energy Moon-forming giant impact. *Sci. Adv.* **4**, eaao5928 (2018).
45. Merle, R. E. et al. Pb–Pb ages and initial Pb isotopic composition of lunar meteorites: NWA 773 clan, NWA 4734, and Dhofar 287. *Meteorit. Planet. Sci.* **55**, 1808–1832 (2020).
46. Černok, A. et al. Preservation of primordial signatures of water in highly-shocked ancient lunar rocks. *Earth Planet. Sci. Lett.* **544**, 116364 (2020).
47. Faircloth, S. J. *Volatiles in the Moon: a Sulfur and Chlorine Perspective*. PhD thesis, Open Univ. (2020).
48. Robinson, K. L. et al. Water in evolved lunar rocks: evidence for multiple reservoirs. *Geochim. Cosmochim. Acta* **188**, 244–260 (2016).
49. McCubbin, F. M. & Barnes, J. J. The chlorine-isotopic composition of lunar KREEP from magnesian-suite troctolite 76535. *Am. Mineral.* **105**, 1270–1274 (2020).
50. McCubbin, F. M. et al. Fluorine and chlorine abundances in lunar apatite: implications for heterogeneous distributions of magmatic volatiles in the lunar interior. *Geochim. Cosmochim. Acta* **75**, 5073–5093 (2011).
51. Hui, H., Peslier, A. H., Zhang, Y. & Neal, C. R. Water in lunar anorthosites and evidence for a wet early Moon. *Nat. Geosci.* **6**, 177–180 (2013).

Acknowledgements

We thank D. Dickens for the provision of AP 007. T.S.H. received funding from an STFC studentship and The Open University (ST/S505614/1). T.S.H. thanks G. Degli-Alessandrini for support in scanning electron microscopy/electron-probe microanalysis work and J. M. Gibson for the collection of O isotopes on AP 007. T.J.B. and T.S.H. also acknowledge support through the Space Strategic Research Area (SRA) funding at The Open University. Additional time for T.S.H. was provided by the CSA Lunar Exploration and Analysis Program (LEAP) awarded to principal investigator G. R. Osinski. A small amount of additional time for T.J.B. was provided by the NASA Solar System Exploration Research Virtual Institute (SSERVI) through a cooperative agreement (80NSSC20M0016, principal investigator D. A. Kring) with the USRA at the LPI in a collaboration between our SSERVI team and a SSERVI international partner. The NordSIMS facility operates as an infrastructure funded by the Swedish Research Council (grant 2021-00371), of which this is publication 739. This work was partially supported by an STFC grant to M.A. and I.A.F. (ST/P000657/1).

Author contributions

T.S.H., M.A., I.A.F. and T.J.B. designed this research. T.S.H. prepared the sample and characterized the petrography and mineral chemistry of AP 007, under guidance from T.J.B. T.S.H., T.J.B. and X.Z. conducted the NanoSIMS measurements and reduced and processed the NanoSIMS data. T.S.H., M.J.W. and H.J. conducted the Pb isotope measurements and reduced and processed the

Pb isotope data. T.S.H. wrote the initial draft of the paper. All authors contributed to the preparation of the final paper.

Competing interests
The authors declare no competing interests.

Additional information
Supplementary information The online version contains supplementary material available at https://doi.org/10.1038/s41550-023-02185-5.

Correspondence and requests for materials should be addressed to Tara S. Hayden.

Peer review information *Nature Astronomy* thanks the anonymous reviewers for their contribution to the peer review of this work.